Hadron collider potential for excited bosons search: A Snowmass whitepaper

M.V. Chizhov^{1,2}, V. A. Bednyakov¹, J. A. Budagov¹

¹ Dzhelepov Laboratory of Nuclear Problems,

Joint Institute for Nuclear Research, 141980, Dubna, Russia

² Centre for Space Research and Technologies,

Faculty of Physics, Sofia University, 1164 Sofia, Bulgaria

The dilepton final states, e^+e^- and $\mu^+\mu^-$, are the most clear channels for new heavy neutral resonances search. Their advantage is that the main irreducible background from the Standard Model Drell–Yan process contributes usually two orders of magnitude lower than the expected signal under the peak region. In this paper we are focused on the search of the excited neutral bosons Z^* . At present only the ATLAS Collaboration is looking for such excitations at LHC. We compare our evaluations with the official collaboration results at 7 TeV, and present our estimations at higher centre-of-mass energies in pp collisions and different luminosities.

PACS numbers: 12.60.-i, 13.85.-t, 14.80.-j

I. INTRODUCTION

The idea of compositeness of the nature is not new. However, in order to explore the internal structure of the matter, the high-energy colliders are necessary. That is why, for example, search of hypothetical excited fermions ψ^* has been fulfilled at all powerful colliders, such as LEP [1], HERA [2], Tevatron [3] and continues at LHC [4, 5].

The excited fermions have anomalous (magnetic moment type) couplings with the known fermions ψ and the gauge bosons (such as gluons, photons and weak W/Z bosons)

$$\mathcal{L}_{\text{excited}}^{\psi^{\star}} = \frac{g}{2\Lambda} \, \bar{\psi}^{\star} \sigma^{\mu\nu} \psi \, \left(\partial_{\mu} Z_{\nu} - \partial_{\nu} Z_{\mu} \right) + \text{h.c.}, \tag{1}$$

where the parameter Λ is connected to the compositeness mass scale of the new physics. Due to their anomalous type of couplings they lead to a unique experimental signature for their detection.

The interaction (1) could be also reinterpreted from a different point of view, introducing the new excited bosons \mathbb{Z}^* [6]

$$\mathcal{L}_{\text{excited}}^{Z^{\star}} = \frac{g}{2\Lambda} \bar{\psi} \sigma^{\mu\nu} \psi \left(\partial_{\mu} Z_{\nu}^{\star} - \partial_{\nu} Z_{\mu}^{\star} \right) \tag{2}$$

instead of the fermionic ones. Such type of new heavy bosons Z^* could also be interesting objects for experimental searches due to their different couplings to the ordinary fermions in comparison with the minimal gauge Z' couplings. In this paper we are focused on the search of the excited bosons Z^* , rather than on the well-known Z' bosons from various benchmark models.

In contrast with the minimal gauge couplings, where either only left-handed or right-handed fermions participate in the interactions, the tensor currents mix both left-handed and right-handed fermions. Therefore, like the Higgs particles, the excited bosons carry a nonzero chiral charge and according to the symmetry of the Standard Model they should be introduced as the electroweak doublets $(Z^* W^*)$ [7] with the internal quantum numbers identical to the Standard Model Higgs doublet.

The existence of such doublets with masses not far from the weak scale is motivated by the hierarchy problem [8]. The effective interaction (2) is induced by quantum loop corrections from a renormalizable underlying theory and represents the lowest order effective Lagrangian for the excited bosons interacting with the Standard Model fermions. The corresponding reference model is described in [9].

Compared to other heavy bosons, interactions mediated by $(Z^* W^*)$ doublets are additionally suppressed in lowenergy processes by powers of small ratio of the momentum transfer to the parameter Λ . Thus, the search of the excited bosons is especially motivated at the LHC and future colliders and at present is conducted by the ATLAS Collaboration [10, 11]. Besides this, the derivative couplings lead to unique signatures for detection of such bosons at the hadron colliders. Decay products of the excited bosons possess previously unexplored angular distribution, which leads to a new strategy of the resonance search and identification in dilepton [12] and dijet [13] channels.

The crucial variable, which can help to differ the decay distribution from other resonances, is an absolute value of the pseudorapidity difference $\Delta \eta \equiv |\eta_1 - \eta_2|$ between the final fermions (see Fig. 1). Decay distributions of all other resonances have the kinematic absolute maximum at $\Delta \eta = 0$, while the excited bosons decay distribution is zero at this point and peaks at $\Delta \eta = \ln(3 + \sqrt{8}) \approx 1.76$. The latter corresponds to the polar angle $\theta = 45^{\circ}$ for the final

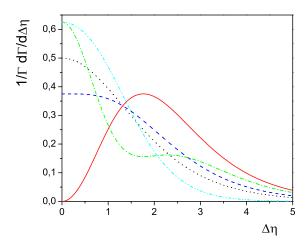


FIG. 1: The normalized angular final fermions distributions as functions of $\Delta \eta$ for the scalar (dotted), spin-1 bosons with the minimal couplings (dashed), the excited bosons (solid) and spin-2 resonances, produced through quark (dash-dotted) and gluon (dash-double-dotted) fusion, are shown.

fermions in the resonance rest frame and a little bit contradicts to the common opinion about an expected signal from new physics at $\theta = 90^{\circ}$.

The background from the Standard Model Drell–Yan (DY) process contributes mainly to the central pseudorapidity region $\Delta \eta \approx 0$ from the intermediate γ/Z bosons, which have the minimal gauge couplings with quarks and leptons. The background can be suppressed up to 40% with appropriate cut $\Delta \eta > \Delta \eta_{\rm min} \approx 1.0$ leaving the main part of the signal intact. This allows to enhance the significance of bump search for the excited bosons in the dilepton channels [12].

However, for dijet final states the huge QCD background is exponentially dominated at high $\Delta \eta$ due to t-channel gluon exchanges, which possess a Rutherford-like distribution $1/(1-\cos\theta)^2$. It is the reason ATLAS and CMS Collaborations to apply severe cut from above $\Delta \eta < \Delta \eta_{\rm max} \approx 1.2 \div 1.3$ [5]. Such low value of $\Delta \eta_{\rm max}$ is optimal for resonance searches with nearly isotropic decay distributions, but is not optimal for the excited bosons, where the most of the signal is removed. Therefore, in order to optimize signal significance for the excited bosons the corresponding cut should be elevated [13] even allowing more background events.

In this paper we investigate hadron collider potential for excited bosons search in the most clear (dilepton) channels. Usually, using these channels leads to more severe constraints on resonance mass than from dijets channels. We compare our evaluations with the official ATLAS Collaboration results at 7 TeV [10], and present our estimations at higher center-of-mass energies in pp collisions and different luminosities.

II. SIGNAL AND BACKGROUND SAMPLES

In order to generate signal and background samples we use the CalcHEP package [14]. Although the package allows to perform calculations only in Born (LO) approximation, using the same generator provides some uniformity between signal and background generation. With its batch and web-interface facilities the CalcHEP has become user-friendly program. Besides this, High Energy Physics Model DataBase (HEPMDB) system [15] and IRIDIS High Performance Computing cluster at the University of Southampton provide access to different theoretical models and fast computer nodes. The authors acknowledge the use of these facilities in the completion of this work.

We have used the simplified reference model ESM [9] for the excited bosons. The only "down-type" neutral Z^* boson interacts both with quarks and charged leptons. Therefore, it can be produced at hadron colliders and can be seen in the leptonic final states in the DY process. To investigate the resonance shape in the invariant dilepton mass and other distributions for various resonance pole masses of Z^* bosons many signal samples should be generated. In this paper we apply a template technique [16] both for signal and background samples. It allows to generate only one sample both for signal and background. The necessary distributions for the fixed pole mass M can be obtained by reweighting the corresponding samples.

The signal template sample is generated without Breit-Wigner pole mass factor

$$BW(m) = \frac{1}{(m^2 - M^2)^2 + (\Gamma M)^2},$$
(3)

and with correction function

$$f(m) = m^{\alpha} \exp(\beta m) \tag{4}$$

of luminosity decreasing at higher dilepton invariant masses m. It can be realized using CalcHEP user function usrFF.c. The latter correction (4) is fulfilled to ensure the same relative errors in reweighted samples regardless of the resonance pole mass. This can be achieved by choosing the constants α and β in such a way that the resulting template distribution decreases inversely with the invariant mass, namely C/m. Therefore, it should be flat in logarithmic invariant mass scale (see Fig. 2).

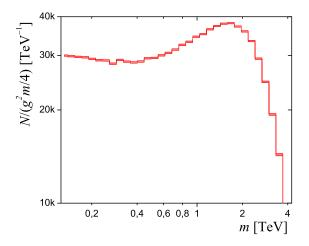


FIG. 2: Z^* template distribution at $\sqrt{s} = 8$ TeV.

Since the total resonance decay width into fermions

$$\Gamma = \frac{g^2}{4\pi} M \approx 0.034M \tag{5}$$

is proportional to the resonance mass, the dimensionless variable x = m/M can be introduced in (3). Then the total number of events and the absolute error after reweighting can be estimated in the resonance vicinity $x \sim 1$ as

$$N_{\text{rew}} \simeq \frac{f^{-1}(M)}{M^4} \int_0^\infty \frac{C dx}{(x^2 - 1)^2 + (g^2/4\pi)^2},$$
 (6)

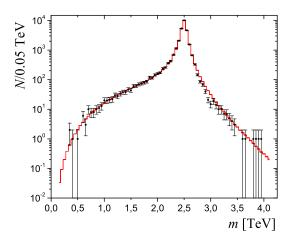
$$\Delta N_{\text{rew}} \simeq \frac{f^{-1}(M)}{M^4} \sqrt{\int_0^\infty \frac{C dx}{[(x^2 - 1)^2 + (g^2/4\pi)^2]^2}}.$$
 (7)

It is valid only for narrow resonances and infinite detector resolution. From eqs. (6) and (7) it is clear that the relative error in the reweighted sample will be approximately the same for any resonance mass from the range $[M_{\min}, M_{\max}]$ and proportional to

$$\frac{\Delta N_{\text{rew}}}{N_{\text{rew}}} \simeq \frac{2}{g} \sqrt{\frac{\ln(M_{\text{max}}/M_{\text{min}})}{N}},$$
 (8)

where N is the total number of generated events in the template sample.

In Fig. 2 the LogFlat signal template distribution at $\sqrt{s} = 8$ TeV is shown, which contains 1 Mevents. The special bin size $g^2m/4 \approx 0.1m$ is selected to show the number of events, which dedicated sample for a fixed pole mass should contain in order to achieve a comparable precision with the reweighted sample from the given template (see eq. (8)).



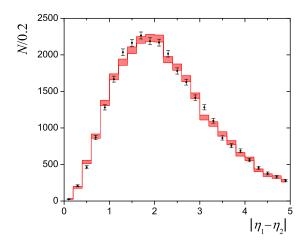


FIG. 3: Comparison between the invariant mass (left) and the pseudorapidity difference (right) distributions for dedicated sample of 2.5 TeV pole mass resonance (points with error bars) and reweighted template sample (histograms) at $\sqrt{s} = 8$ TeV is shown.

To validate this statement a comparison between distributions for dedicated sample of 2.5 TeV pole mass resonance produced at $\sqrt{s} = 8$ TeV containing 30 kevents and reweighted template sample is shown in Fig. 3.

To derive the exclusion limits and the discovery potential we should compare the signal and the background. In this paper the simplest "number counting" approach is adopted, which is based on the comparison of the expected rate of events for the signal and the background processes. From these rates, and assuming Poisson statistics, one can determine the probability that background fluctuations produce a signal-like result according to some estimator, e.g. the likelihood ratio.

For the narrow resonances the bulk of events populates the vicinity around the peak $[M - k\Gamma, M + k\Gamma]$. The relative ratio of the signal events in this region to the total events number can be estimated using eq. (3) as

$$s = \frac{2\arctan(k)}{\pi}.\tag{9}$$

If we assume that the background contribution is proportional to the size of the on-peak region $b \sim k$, we can estimate analytically the maximum of the signal significance on k using the formula from Appendix A of Ref. [17]

$$S_{CL} = \sqrt{2\left((s+b)\ln\left(1+\frac{s}{b}\right) - s\right)},\tag{10}$$

which follows directly from the Poisson distribution. We will use this equation for estimation of discovery potential. The corresponding curves as a function of the window size are shown in Fig. 4. The middle curve reaches maximum at $k \simeq 3$ for $s/b \simeq 43.8$, which corresponds, for example, to resonance production with M=3.25 TeV at $\sqrt{s}=8$ TeV. The upper and bottom curves correspond to 10 times bigger and lower signal to background ratios, respectively. They reach maxima at a little bit bigger and lower size windows than the middle curve, correspondingly. It is in a good agreement with the numerical calculations (see Fig. 2 from [18]). In the following we will use the optimal average value k=3.

However, in the muon channel the experimental $p_{\rm T}$ resolution increases as $p_{\rm T}^2$ at high muon momenta. It means that at some point we cannot neglect anymore the experimental resolution in comparison with resonance width, which increases linearly with resonance mass (see eq. (5)). Therefore, in this case we cannot choose the optimal window due to experimental resolution and oblige to increase it allowing more background, that directly affects the discovery potential and the exclusion limits in the muon and combined channels. We are thankful to Igor Boyko for this remark.

III. EXCLUSION LIMITS AT $\sqrt{s} = 7$ TEV AND COMPARISON WITH ATLAS RESULTS.

At present only the ATLAS Collaboration is looking for a production of the excited Z^* bosons [10, 19]. In 2011 the ATLAS Collaboration collected 4.9 fb⁻¹ of an integrated luminosity in dielectron channel and 5.0 fb⁻¹ in dimuon

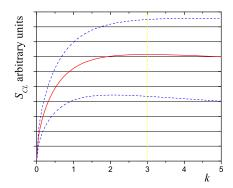


FIG. 4: The signal significance curves for different signal to background ratios as a function of the window size.

channel at a center-of-mass energy of 7 TeV. The 95% CL observed and the expected exclusion limits are shown in Table I [10].

	$Z^{\star} \rightarrow \mu^{+}\mu^{-}$	$Z^{\star} \rightarrow e^{+}e^{-}$	$Z^{\star} \to \ell^+ \ell^-$
Observed limit [TeV]	1.97	2.10	2.20
Expected limit [TeV]	1.99	2.13	2.22

TABLE I: The observed and expected 95% CL lower limits on the mass of the Z^* boson for the $\mu^+\mu^-$ and e^+e^- channels separately and for their combination from [10].

The combination of the dielectron and dimuon channels is performed under the assumption of lepton universality. The combined limit on the cross section times branching fraction (σBr) expected from theory is around 0.7 fb and can be read from Fig. 4 of [10]. Since there are no events above 2 TeV dilepton invariant mass and the background is very small, the observed and expected limits are nearly the same.

The ATLAS Collaboration has used the Bayesian approach [20] with a flat, positive prior on the signal cross section to determine an upper limit on the number of signal events. In this paper we will use more simple "number counting" approach for the exclusion limit and the discovery potential evaluations with many other approximations. Nevertheless, we will show that our limit estimations are in agreement with the official ATLAS results.

Since there is not yet a deviation from the Standard Model distributions only the exclusion limits can be evaluated. To do this we will use an approximate computation of the confidence level for combining searches with small statistics [21]. The $[M-k\Gamma,M+k\Gamma]$ on-peak region with k=3 has been used for event counting in both channels for the resonance masses below 2 TeV. However, due to bad experimental resolution in the muon channel for the resonance masses above 2 TeV we assume k=3M[TeV]/2 TeV. We will take into an account only the leading Z/γ DY background and neglect many subdominant backgrounds, like QCD, $t\bar{t}$, diboson and W+ jets.

The number of the expected events, recorded in the detector and that have passed a selection criteria, depends on many factors, which can be expressed through the overall event acceptance times efficiency ($A\epsilon$). So, for a Z' boson of mass 2 TeV decaying into a dielectron final state the overall event $A\epsilon$ is about 66%, while for the muon channel this factor is only 43% for the ATLAS detector during 2010 data taking period [19]. To be specific, we will accept the following rounded overall event $A\epsilon$ numbers for the ATLAS detector: 70% for the electron channel and 40% for the muon channel, both for signal and background.

In order to follow closely as possible the ATLAS analysis in this section we will use the same PDF set, CTEQ6L1 [22], used by ATLAS for signal generation. Since only the central value is available for the CTEQ6L1 PDF set, the closest set, CTEQ61 [23], is used to estimate systematic PDF uncertainties (see Table II).

The PDF uncertainties dominate at high dilepton invariant masses. Therefore, we will use only them as systematic uncertainties. Using program eclsyst.f [21] we get the following limits on Z^* mass: 2.01 TeV in the muon channel and 2.15 TeV in the electron channel. Their combination excludes at 95% confidence level Z^* masses below 2.25 TeV and $\sigma Br > 0.7$ fb. The obtained results are very close to the official ATLAS results and convince us to investigate the LHC potential at higher center-of-mass energies.

Z	* mass	signal		background		Z^* mass	signal		background	
	[GeV]	σBr [fb]	$\Delta\sigma/\sigma~[\%]$	σBr [fb]	$\Delta\sigma/\sigma~[\%]$	[TeV]	σBr [ab]	$\Delta\sigma/\sigma~[\%]$	σBr [ab]	$\Delta\sigma/\sigma$ [%]
	250	64866.	5.1	355.66	4.4	2.00	1565.2	32.1	15.248	17.5
	500	4608.2	7.0	25.418	5.4	2.25	507.93	41.9	5.8910	22.1
	750	779.58	9.5	4.5352	6.4	2.50	165.43	54.8	2.3148	27.7
	1000	184.29	11.9	1.1399	7.4	2.75	53.988	72.0	0.91438	34.5
	1250	51.121	15.4	0.34161	8.4	3.00	17.720	93.3	0.35945	42.8
	1500	15.436	19.3	0.11385	10.7	3.25	5.8534	118.4	0.13933	53.1
	1750	4.8631	24.9	0.040702	13.6	3.50	1.9359	146.6	0.052909	65.8

TABLE II: Z^* signal and the Standard Model DY background cross sections times branching fraction in $[M-3\Gamma, M+3\Gamma]$ on-peak region and maximal relative uncertainty due to PDF variation (at 90% C.L.) with CTEQ61 set.

IV. EXCLUSION LIMITS AT $\sqrt{s} = 8$ TEV.

In 2012 the ATLAS experiment recorded 20 fb⁻¹ of good data both in electron and muon channels at $\sqrt{s} = 8$ TeV. Again good agreement between the data and the background expectation was found [24]. However, limits only on the Z' Sequential Standard Model boson, E_6 gauge bosons and a spin-2 Randall-Sundrum graviton have been set so far. There are still no events observed by ATLAS [24] above 2 TeV dilepton invariant mass and the observed and expected limits are nearly the same.

In this paper we precede the official ATLAS results on the excited boson search and evaluate exclusion limits on \mathbb{Z}^* at $\sqrt{s}=8$ TeV. The analysis is fulfilled in the same lines as in the previous section. The only difference, that we will use more recent MSTW2008lo PDF set [25] for signal and background generation. The corresponding PDF systematics are presented in Table III.

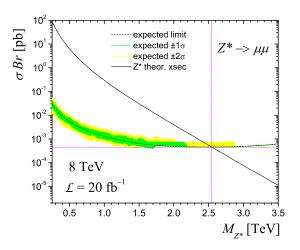
Z^* mass	signal		background		Z^*	mass	signal		background	
[GeV]	σBr [fb]	$\Delta\sigma/\sigma$ [%]	σBr [fb]	$\Delta\sigma/\sigma~[\%]$		[TeV]	σBr [ab]	$\Delta\sigma/\sigma~[\%]$	σBr [ab]	$\Delta \sigma / \sigma \ [\%]$
250	75011.	3.1	408.12	2.5		2.25	1341.4	16.6	14.809	13.7
500	5657.3	4.2	30.944	3.4		2.50	492.04	19.8	6.4583	16.3
750	1044.4	5.5	6.0493	4.3		2.75	179.93	23.5	2.8387	19.5
1000	272.90	6.9	1.6845	5.3		3.00	65.599	28.2	1.2481	22.8
1250	84.302	8.7	0.56248	6.5		3.25	23.814	33.1	0.54635	26.2
1500	28.493	10.3	0.20889	7.8		3.50	8.6385	37.4	0.23602	29.7
1750	10.090	12.0	0.083116	9.4		3.75	3.1289	40.6	0.10036	33.3
2000	3.6597	14.2	0.034575	11.3		4.00	1.1286	42.0	0.041827	36.8

TABLE III: Z^* signal and the Standard Model DY background cross sections times branching fraction in $[M-3\Gamma, M+3\Gamma]$ on-peak region and relative uncertainty due to PDF variation (at 90% C.L.) with MSTW2008lo90cl set.

Figure 5 shows the 95% C.L. expected exclusion limits on σBr for the electron and muon channels. The combined limit is shown in Fig. 6. Table IV summarizes the constraints on the resonance mass and σBr of \mathbb{Z}^* boson.

Expected limit	$Z^{\star} \to \mu^{+}\mu^{-}$	$Z^{\star} \rightarrow e^{+}e^{-}$	$Z^{\star} \to \ell^+ \ell^-$
M [TeV]	2.55	2.67	2.80
σBr [fb]	0.45	0.27	0.17

TABLE IV: The expected 95% CL limits on the mass and the cross section times branching fraction of the Z^* boson for the $\mu^+\mu^-$ and e^+e^- channels separately and for their combination at $\sqrt{s}=8$ TeV.



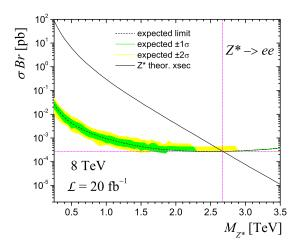


FIG. 5: Exclusion limits from muon (left) and electron (right) channels with 20 fb⁻¹ of integrated luminosity at $\sqrt{s} = 8$ TeV.

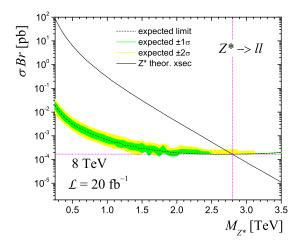


FIG. 6: Combined exclusion limits with 20 fb⁻¹ of integrated luminosity at $\sqrt{s} = 8$ TeV.

V. THE DISCOVERY POTENTIAL AND THE EXCLUSION LIMITS AT $\sqrt{s}=13$ TEV AND $\sqrt{s}=14$ TEV.

In 2015 the LHC will increase the center-of-mass energy up to the design value. In this section we will estimate the discovery potential and the exclusion limit, if no deviation from the Standard Model will be observed. For discovery potential estimation we use eq. (10) with $S_{CL} = 5$. At the first stage the center-of-mass energy could be 13 TeV. Therefore, we will consider first this possibility.

The corresponding cross sections and PDF systematic uncertainties are presented in Table V.

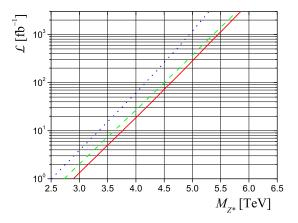
Depending on the luminosity they give the following results shown in Fig. 7. It is interesting to note that higher center-of-mass energy at Run 2 allows to probe higher resonance masses than at Run 1 already with 1 fb^{-1} of an integrated luminosity.

The designed $\sqrt{s} = 14$ TeV requires new templates and systematics (see Table VI), which only slightly deviates from the previous case.

The final results are presented in Fig. 8. In particular, LHC Run 2 can discover Z^* up to about 5.3 TeV or exclude it in case of signal absence up to resonance masses of 5.5 TeV. The High Luminosity LHC with 3000 fb⁻¹ of an integrated luminosity can extend that reach in case of a signal to about 6.2 TeV for discovery or exclude it up to about 6.4 TeV.

Z^* mass	signal		background		Z^* mass	signal		background	
[TeV]	σBr [ab]	$\Delta\sigma/\sigma~[\%]$	σBr [ab]	$\Delta\sigma/\sigma~[\%]$	[TeV]	σBr [zb]	$\Delta\sigma/\sigma~[\%]$	σBr [zb]	$\Delta\sigma/\sigma$ [%]
2.0	32645.	8.5	217.26	6.4	4.5	56554.	25.4	914.46	19.9
2.5	8500.8	10.6	63.858	8.1	5.0	16214.	32.5	330.30	24.0
3.0	2369.6	12.9	20.720	10.2	5.5	4635.1	40.6	117.88	28.3
3.5	679.60	15.8	7.1252	12.8	6.0	1321.1	49.2	41.176	32.6
4.0	196.25	19.9	2.5343	16.1	6.5	375.23	57.8	13.968	36.9

TABLE V: Z^* signal and the Standard Model DY background cross sections times branching fraction in $[M-3\Gamma, M+3\Gamma]$ on-peak region and relative uncertainty due to PDF variation (at 90% C.L.) with MSTW2008lo90cl set at $\sqrt{s}=13$ TeV.



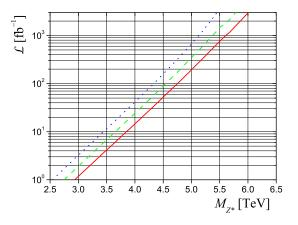
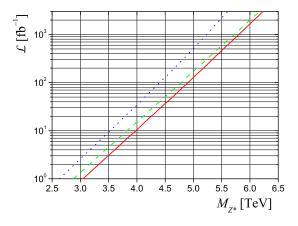


FIG. 7: Discovery potential (left) and expected 95% CL exclusion limits (right) at $\sqrt{s} = 13$ TeV from muon (dotted), electron (dashed) and combined (solid) channels.



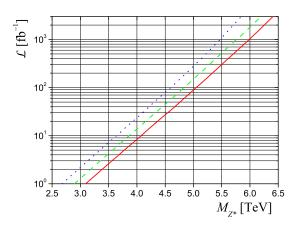


FIG. 8: The discovery potential (left) and the expected 95% CL exclusion limits (right) at $\sqrt{s} = 14$ TeV from muon (dotted), electron (dashed) and combined (solid) channels.

VI. THE DISCOVERY POTENTIAL AND THE EXCLUSION LIMITS AT $\sqrt{s}=33$ TEV.

At the end of the paper we will investigate also the discovery potential and the exclusion limits for the excited boson search in the case of the highest center-of-mass energy, $\sqrt{s} = 33$ TeV.

The corresponding data are given in Table VII.

The discovery potential and the exclusion limits on the excited boson resonance mass depending on the integrated

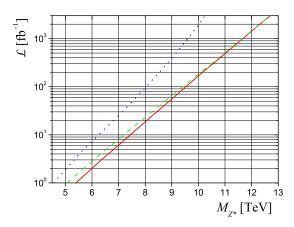
2	Z* mass	signal		background		Z^* mass	mass signal		background	
	[TeV]	σBr [ab]	$\Delta\sigma/\sigma~[\%]$	σBr [ab]	$\Delta\sigma/\sigma$ [%]	[TeV]	σBr [zb]	$\Delta\sigma/\sigma~[\%]$	σBr [zb]	$\Delta\sigma/\sigma~[\%]$
	2.5	11603.	9.8	83.291	7.5	5.0	33566.	25.8	580.80	21.1
	3.0	3471.3	11.8	28.383	9.3	5.5	10502.	31.2	225.02	24.9
	3.5	1.0776	14.1	10.295	11.5	6.0	3279.4	36.4	86.134	28.9
	4.0	339.13	17.1	3.8814	14.2	6.5	1022.9	40.1	32.344	32.9
	4.5	106.88	20.9	1.4963	17.4	7.0	317.37	41.5	11.820	36.9

TABLE VI: Z^* signal and the Standard Model DY background cross sections times branching fraction in $[M-3\Gamma, M+3\Gamma]$ on-peak region and relative uncertainty due to PDF variation (at 90% C.L.) with MSTW2008lo90cl set at $\sqrt{s} = 14$ TeV.

Z^*	mass	signal		background		Z^* n	nass	signal		background	
	[TeV]	σBr [ab]	$\Delta\sigma/\sigma~[\%]$	σBr [ab]	$\Delta\sigma/\sigma~[\%]$	[]	[eV]	σBr [zb]	$\Delta\sigma/\sigma~[\%]$	σBr [zb]	$\Delta\sigma/\sigma$ [%]
	4.5	8741.9	7.7	56.12	5.7		9.5	48328.	17.5	570.54	14.6
	5.5	2824.5	9.3	19.769	7.0		10.5	17979.	20.9	251.65	17.4
	6.5	979.46	10.9	7.6047	8.4		11.5	6681.0	24.9	111.70	20.4
	7.5	353.68	12.7	3.0997	10.1		12.5	2476.7	29.4	49.630	23.7
	8.5	130.17	14.9	1.3131	12.1		13.5	915.92	33.9	21.899	27.0

TABLE VII: Z^{\star} signal and the Standard Model DY background cross sections times branching fraction in $[M-3\Gamma, M+3\Gamma]$ on-peak region and relative uncertainty due to PDF variation (at 90% C.L.) with MSTW2008lo90cl set at $\sqrt{s}=33$ TeV.

luminosity are presented in Fig. 9. The plots show that High Energy LHC can probe around two times heavier



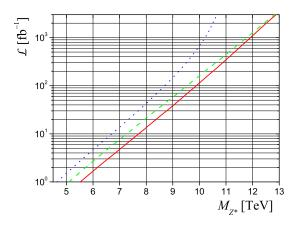


FIG. 9: The discovery potential (left) and the expected 95% CL exclusion limits (right) at $\sqrt{s} = 33$ TeV from muon (dotted), electron (dashed) and combined (solid) channels.

resonance masses at the same integrated luminosities than at Run 2.

VII. CONCLUSION

In this paper we have considered the discovery potential and the exclusion limits on the excited boson search in pp collisions at the LHC for the different center-of-mass energies and different luminosities. In particular, LHC Run 2 can discover Z^* up to about 5.3 TeV, while the High Luminosity (HL) LHC can extend that reach to about 6.2 TeV. The High Energy (HE) LHC can probe around two times heavier resonance masses at the same integrated luminosities.

The field for Z^* search remains opened both at the HL-LHC and the HE-LHC.

- R. Barate et al. (ALEPH Collaboration), Eur. Phys. J. C 4, 571 (1998); G. Abbiendi et al. (OPAL Collaboration), Phys. Lett. B 544, 57 (2002); P. Achard et al. (L3 Collaboration), Phys. Lett. B 568, 23 (2003); J. Abdallah et al. (DELPHI Collaboration), Eur. Phys. J. C 46, 277 (2006).
- [2] C. Adloff et al. (H1 Collaboration), Phys. Lett. B 548, 35 (2002); S. Chekanov et al. (ZEUS Collaboration), Phys. Lett. B 549, 32 (2002).
- [3] D. Acosta et al. (CDF Collaboration), Phys. Rev. Lett. 94, 101802 (2005); V. M. Abazov et al. (D0 Collaboration) arXiv:0801.0877 [hep-ex].
- [4] ATLAS Collaboration, NJP 15 (2013) 093011, arXiv:1308.1364 [hep-ex]; CMS Collaboration, Phys. Lett. B 720 (2013) 309, arXiv:1210.2422 [hep-ex].
- [5] ATLAS Collaboration, Phys. Lett. B 708 (2012) 37, arXiv:1108.6311 [hep-ex]; CMS Collaboration, Phys. Rev. D 87 (2013) 114015, arXiv:1302.4794 [hep-ex].
- [6] M.V. Chizhov, V.A. Bednyakov, J.A. Budagov, Phys. Atom. Nucl. 71 (2008) 2096-2100, arXiv:0801.4235 [hep-ph].
- [7] M.V. Chizhov, Mod. Phys. Lett. A 8 (1993) 2753-2762, hep-ph/0401217; hep-ph/0609141.
- [8] M.V. Chizhov, Gia Dvali, Phys. Lett. B703 (2011) 593-598, arXiv:0908.0924 [hep-ph].
- [9] M.V. Chizhov, Phys. Part. Nucl. Lett. 8 (2011) 512-516, arXiv:1005.4287.
- [10] ATLAS Collaboration, JHEP 11 (2012) 138, arXiv:1209.2535 [hep-ex].
- [11] ATLAS Collaboration, Eur. Phys. J. C72 (2012) 2241, arXiv:1209.4446 [hep-ex].
- [12] M.V. Chizhov, V.A. Bednyakov, J.A. Budagov, Phys. Part. Nucl. Lett. 10 (2013) 144-146, arXiv:1109.6876 [hep-ph].
- [13] M.V. Chizhov, V.A. Bednyakov, J.A. Budagov, Phys. Atom. Nuclei 75 (2012) 90; arXiv:1106.4161 [hep-ph].
- [14] A. Belyaev, N.D. Christensen, A. Pukhov, Comput. Phys. Commun. 184 (2013) 1729-1769, arXiv:1207.6082 [hep-ph].
- [15] M. Bondarenko, A. Belyaev, L. Basso, E. Boos, V. Bunichev *et al.*, "High Energy Physics Model Database: Towards decoding of the underlying theory" (within "Les Houches 2011: Physics at TeV Colliders New Physics Working Group Report"), arXiv:1203.1488 [hep-ph], https://hepmdb.soton.ac.uk
- [16] C.P. Hays, A.V. Kotwal, O. Stelzer-Chilton, Mod. Phys. Lett. A24 (2009) 2387-2403, arXiv:0910.1770 [hep-ex].
- [17] G.L. Bayatian et al., (CMS Collaboration), J. Phys. G34 (2007) 995.
- [18] M.V. Chizhov, V.A. Bednyakov, J.A. Budagov, Nuovo Cim. C33 (2010) 343-350, arXiv:1005.2728 [hep-ph].
- [19] ATLAS Collaboration, Phys. Lett. B700 (2011) 163-180, arXiv:1103.6218 [hep-ex].
- [20] A. Caldwell, D. Kollar, K. Kroninger, Comput. Phys. Commun. 180 (2009) 2197, arXiv:0808.2552 [physics.data-an].
- [21] T. Junk, Nucl. Instrum. Meth. A434 (1999) 435-443, hep-ex/9902006.
- [22] J. Pumplin et al., JHEP 07 (2002) 012, hep-ph/0201195.
- [23] D. Stump et al., JHEP 10 (2003) 046, hep-ph/0303013.
- [24] ATLAS Collaboration, ATLAS-CONF-2013-017.
- [25] A.D. Martin et al., Eur. Phys. J. C63 (2009) 189-285, arXiv:0901.0002 [hep-ph].